

# MULTI-DIMENSIONAL MODULATION CODES FOR FADING CHANNEL

*GRANT  
1N-32-CR  
46465  
P.33*

Technical Report

to

NASA

Goddard Space Flight Center

Greenbelt, Maryland 20771

Grant Number NAG 5-931

Report Number NASA 91-003

Shu Lin

Principal Investigator

Department of Electrical Engineering

University of Hawaii at Manoa

Honolulu, Hawaii 96822

October 10, 1991

(NASA-CR-188959) MULTI-DIMENSIONAL  
MODULATION CODES FOR FADING CHANNEL (Hawaii  
Univ.) 33 p CSCL 20N

N91-32288

Unclas  
G3/32 0046465

# Multi-dimensional Modulation Codes for Fading Channel

Jiantian Wu    Shu Lin

## Abstract

In this paper, we present some new codes which have good performance on Rician fading channel with small decoding complexities. First, we propose a new  $M$ -way partition chain for the  $L \times MPSK$  ( $L \leq M$ ) signal set which maximizes the intra-set distance of each subset at each partition level. Based on this partition chain, a class of asymptotical optimum codes has been found. For  $M = 4$ , these codes have both large symbol distances and product distances.

Multi-level coding scheme allows us to construct a code by hand such that the code meets some desired parameters, e.g., symbol distance, product distance, etc. In design of a multi-level code, we consider all factors which affect the performance and complexity of the code, such as, the decoding scheme, decoding complexity and performance under the decoding scheme, e.g., if the multi-stage decoding scheme is used, the performance degradation due to the suboptimum decoding is taken into consideration. The performance for most of the codes presented in this paper has been simulated on Rayleigh fading channel, and the results show that these codes have good performance with small decoding complexities.

# 1 Introduction

In the conventional communication systems, coding and modulation are considered as two independent segments. Engineers who designed one segment might not know the other segment at all. In such system, each segment might be optimized, but the whole system is far from optimum. Massey pointed out that a significant improvement can be achieved if the channel coding and modulation are considered together[1] and designed as a single entity. Later, Ungerboeck presented a method to combine trellis coding with modulation using “mapping by set partitioning” technique [2]. This method is now known as trellis coded modulation (TCM) and is widely used in today’s data communication systems.

The original TCM is used for additive white Gaussian noise (AWGN) channel. The trellis code is designed to maximum the Euclidean distance between code sequences transmitted on the channel. Divsalar and Simon studied the TCM on fading channel. They found that the design criteria of codes for fading channel is different from that for AWGN channel[4-6]. Similar results have been obtained by others [7-9]. In this paper, we investigate multi-dimensional trellis codes for fading channel.

For simplicity, we consider the non-selective slow Rician fading channel with perfect phase tracking. The analytical model of the channel is shown in Figure 1. We denote a coded sequence of length  $N$  by

$$\underline{x} = (x_1, x_2, \dots, x_N) \quad (1)$$

where the  $k$ th element of  $\underline{x}$ ,  $x_k$ , represents the transmitted MPSK symbol in the  $k$ th transmission interval. In phase notation,  $x_k$  can be written as

$$x_k = \sqrt{2}E_s e^{j\phi_k} \quad (2)$$

where  $E_s$  is the energy per MPSK symbol.  $E_s$  can be expressed as  $E_s = R \cdot E_b$ , where  $R$  is the information rate (i.e., the number of information bits per coded symbol) and  $E_b$  is the energy per information bit.

Corresponding to  $\underline{x}$ , the received signal sequence

$$\underline{y} = (y_1, y_2, \dots, y_N) \quad (3)$$

can be expressed as

$$y_k = a_k x_k + n_k \quad (4)$$

where  $a_k$  is the multiplicative distortion introduced by the fading, and  $n_k$  is a two-dimensional Gaussian random vector with one-sided noise density  $N_0$ . In this study, we assume that  $a_k$  has the following probability density function (*p.d.f.*):

$$p(a_k) = 2a_k e^{a_k^2(1+K)-K} I_0(2a_k \sqrt{K}(K+1)), \quad a_k \geq 0 \quad (5)$$

where  $K$  is the ratio of powers of the steady to diffuse fading signal components,  $I_0(\bullet)$  is the zero order modified Bessel function of the first kind and  $E[a_k^2] = 1$  assuming the received signal energy is equal to the transmitted signal energy  $E_s$ . The mean and the variance of the random variable  $a_k$  are given by

$$m_a = \frac{1}{2} \sqrt{\frac{\pi}{1+K}} e^{-K/2} ((1+K)I_0(K/2) + KI_1(K/2)) \quad (6)$$

$$\sigma_a^2 = 1 - m_a^2 \quad (7)$$

respectively, where  $I_1(\bullet)$  is the first order modified Bessel function. Small values of  $K$  indicate a severely fading, and the Rayleigh fading is a special case for  $K = 0$  (no steady signal component). Large values of  $K$  indicate a slight fading, and the AWGN channel is a special case for  $K = \infty$ .

The interleaving is an important technique for fading channels, and the interleaving depth must be finite in any practical system. For convenience, however, we assume

that the interleaving depth is infinite. Based on the above assumption, an upper bound can be obtained by computing the pair-wise error probability bound. Suppose  $\underline{x}$  is the transmitted sequence, and the metric used in decoding is the squared Euclidean distance (SED), i.e., the code sequence with smallest SED from the received sequence is decoded as the transmitted code sequence. If the decoded sequence is  $\hat{\underline{x}}$  instead of  $\underline{x}$ , the code (path)  $\hat{\underline{x}}$  is called an error path, and the pair-wise error probability is equal to

$$P(\underline{x} \rightarrow \hat{\underline{x}}) = Pr \{m(\underline{y}, \hat{\underline{x}}) < m(\underline{y}, \underline{x})\} \quad (8)$$

where  $m(\bullet, \bullet)$  is the metric function, i.e., the SED in this case. To describe the upper bound, we define the following parameters. The *squared Euclidean distance* between  $\hat{\underline{x}}$  and  $\underline{x}$  is given by

$$d^2(\hat{\underline{x}}, \underline{x}) = \sum_{i=1}^N |\hat{x}_i - x_i|^2 \quad (9)$$

The *symbol (Hamming) distance* between sequences  $\hat{\underline{x}}$  and  $\underline{x}$  denoted by  $\delta_H(\hat{\underline{x}}, \underline{x})$  is the number of different symbols between the two sequences. The *symbol distance* of the code, denoted by  $\delta_H$ , is defined as the minimum symbol distance between any two code sequences. The *product distance (PD)* between  $\hat{\underline{x}}$  and  $\underline{x}$  denoted by  $\Delta_p(\hat{\underline{x}}, \underline{x})$  is defined as the product of the corresponding nonzero squared Euclidean symbol distances between  $\hat{\underline{x}}$  and  $\underline{x}$ :

$$\Delta_p^2(\hat{\underline{x}}, \underline{x}) = \prod_{\substack{k=1 \\ x_k \neq \hat{x}_k}}^N |x_k - \hat{x}_k|^2 \quad (10)$$

The *product distance* of the code is the minimum product distance between a pair of code sequences with symbol distance  $\delta_H$ . The pair-wise error probability of choosing the code sequence  $\hat{\underline{x}}$  instead of  $\underline{x}$  can be computed in terms of the symbol distance, the squared Euclidean distance and the product distance. Large symbol distance needs

large number of states in the trellis diagram of the code, which leads to very complex and expensive decoder. Therefore, we only consider the codes with moderate symbol distances. There are two cases in terms of the availability of channel information. First, we consider the case that the channel state information is not available. For large signal-to-noise ratio (SNR), the pair-wise error probability of choosing the code sequence  $\hat{\underline{x}}$  instead of  $\underline{x}$  can be expressed as [8]

$$P(\underline{x} \rightarrow \hat{\underline{x}}) = P_{d,\delta,\Delta} \leq \frac{(\sqrt{8}\sigma d)^{2\delta_H(\hat{\underline{x}},\underline{x})}}{2\Delta_p^2(\hat{\underline{x}},\underline{x})} \quad (11)$$

where  $d$  is the Euclidean distance between the two code words.

Second, if the channel state information (CSI) is available, that is, the fading attenuation  $a_k$  at time  $k$  is known, the branch metric in CSI decoding is

$$m_k = |y_k - a_k x_k|^2 \quad (12)$$

The pair-wise error probability of choosing the code sequence  $\hat{\underline{x}}$  instead of  $\underline{x}$  can be expressed as [8]

$$P(\underline{x} \rightarrow \hat{\underline{x}}) = P_{d,\delta,\Delta} \leq \frac{(8\sigma^2 d^2 (1+K)e^{-K})^{\delta_H(\hat{\underline{x}},\underline{x})}}{2\Delta_p^2(\hat{\underline{x}},\underline{x})} \quad (13)$$

In both cases, an upper bound on the average bit error probability is obtained from the pair-wise error probability bound as

$$P_b \leq \sum_{\hat{\underline{x}}, \underline{x} \in C} b(\hat{\underline{x}}, \underline{x}) p(\underline{x}) P(\underline{x} \rightarrow \hat{\underline{x}}) \quad (14)$$

where  $b(\hat{\underline{x}}, \underline{x})$  is the number of bit errors that occur when  $\underline{x}$  is transmitted and  $\hat{\underline{x}}$  is chosen by the decoder,  $p(\underline{x})$  is the a priori probability of transmitted  $\underline{x}$  and  $C$  is the set of all coded sequences. The upper bound given by (14) can be evaluated by the distance spectrum of the code.

Denote  $A(d, \delta, \Delta)$  as the average number of code sequence pairs  $\underline{x}, \underline{\hat{x}}$  with Euclidean distance  $d$ , symbol distance  $\delta$  and product distance  $\Delta$ . The parameter  $A(d, \delta, \Delta)$  is called the average *multiplicity* of the code. For fading channels, a spectral line is defined by Euclidean distance  $d$ , symbol distance  $\delta$ , product distance  $\Delta$ , and an average multiplicity  $A(d, \delta, \Delta)$ . The set of all spectral lines of a code is called the *distance spectrum* of that code.

Using the distance spectrum of the code, the above bound can be written as

$$P_b \leq \frac{1}{R} \sum_{d, \delta, \Delta} b_{d, \delta, \Delta} A(d, \delta, \Delta) P_{d, \delta, \Delta} \quad (15)$$

where  $b_{d, \delta, \Delta}$  is the average number of erroneous information bits on a path characterized by the Euclidean distance  $d$ , symbol distance  $\delta$  and product distance  $\Delta$ , and  $R$  is the number of information bits per coded symbol.

The upper bound provides a guidance for the design of codes for a fading channel. The symbol distance is the most important parameter. It determines the rate of the decrease of error probability. The bit error probability of a decoded sequence by Viterbi decoding is inversely proportional to the product distance of the code. Both symbol distance and product distance should be as large as possible, and they play different roles on the performance of the code. At low SNR, the product distance is more important, whereas at high SNR, the symbol distance becomes more important, which dominates the asymptotic behavior of the code. Apart from these two parameters, the path multiplicity is also an important factor. To design a good code for practical use, we have to set these parameters at reasonable values. We will see that a code with maximized symbol distance and extremely small product distance is not a good code.

## 2 Multidimensional Trellis Codes with Maximized Symbol Distance

Optimum two dimensional trellis codes have been found by computer search [7]. Divsalar and Simon pointed out that multidimensional trellis codes have performance/complexity advantage over two-dimensional trellis codes for fading channel[5]. They also showed that the Ungerboeck's set partition chain is not optimum for designing multi-dimensional trellis codes for fading channels. They found that, by properly partitioning multi-dimensional signal sets, trellis codes with symbol distance larger than or equal to 2 can be easily found by hand. Codes presented in their papers [4-6] have small numbers of states with either symbol distance 2 and information rate equal to 2 bits/symbol or symbol distance larger than 2 and information rate less than 2 bits/symbol. In this paper, we present codes with small number of states and either higher information rate or better performance (larger symbol distance and product distance). In this section, we discuss the trellis codes with maximized symbol distances.

We use a set  $\{0, 1, \dots, M - 1\}$  to express the set of MPSK signal points by the natural labelling as shown in Figure 2 for the case  $M = 8$ . Denote  $(n, k, d_H, q)$  as a code over  $GF(q)$  with block length  $n$ , number of information symbols  $k$  and minimum Hamming distance  $d_H$  ( $q$  is omitted if  $q = 2$ ).

It is obvious that a code with maximum symbol distance is the code with maximum minimum Hamming distance as long as we regard a point in MPSK signal set as an element in  $GF(M)$ . For any signal set of MPSK, let  $\psi = \{0, 1, \dots, M - 1\} \rightarrow GF(M)$

be a one-to-one map, e.g.,

$$\begin{aligned}\psi(0) &= 0, \\ \psi(i) &= \alpha^{i-1}, \quad i = 1, 2, \dots, M-1,\end{aligned}\tag{16}$$

where  $\alpha$  is a primitive element of  $GF(M)$ . Then the symbol distance between any two vectors in  $2L$  dimensional MPSK signal set ( $L \times$  MPSK) is equal to the minimum Hamming distance between any corresponding vectors  $\underline{c}_1$  and  $\underline{c}_2$  over  $GF^L(M)$ . Thus, to obtain an optimum partition chain for the  $L \times$  MPSK signal set in terms of symbol distance is equivalent to design an optimum partition chain of  $GF^L(M)$  in terms of Hamming distance. In [11], it has been shown that, for  $L \leq M$ , there exists a partition chain  $GF^L(M) = RS(L, L)/RS(L, L-1)/\dots/RS(L, 1)/\{0\}$  with Hamming distances  $1/2/\dots/L/\infty$ , where  $0$  is the all-zero vector in  $GF^L(M)$  and  $RS(L, K)$  is the Reed-Solomon code (extended for  $L = M$ , or shortened for  $L < M - 1$ ) over  $GF(M)$  of length  $L$  and number of information symbols  $K$ . Therefore, we can use these set partition chains to construct trellis codes with high information rates and large symbol distances. The following is a brief description of the expression of set partition chain  $GF^L(M) = RS(L, L)/RS(L, L-1)/\dots/RS(L, 1)/\{0\}$ .

Let  $A_i = RS(L, L-i)$ ,  $i = 0, 1, \dots, L-1$ , and  $A_L = \{0\}$ . Then  $A_{i+1}$  partitions  $A_i$  into  $M$  cosets. Denote  $[A_i/A_{i+1}]$  as the set of coset representatives of  $A_{i+1}$  in  $A_i$ , for  $i = 0, 1, \dots, L-1$ . Due to the linearity of the codes  $A_i$ ,  $i = 0, 1, \dots, M$ , the partition can be expressed as

$$A_i = \bigcup_{g^{(i)} \in GF(M)} (g^{(i)} \underline{a}_i + A_{i+1}), \text{ for } i = 0, 1, \dots, L-1,\tag{17}$$

where  $\underline{a}_i$  is a coset representative of  $A_{i+1}$  in  $A_i$ . Thus every codeword in  $A_0$  can be completely expressed by the set of  $M$ -ary numbers  $g^{(0)}g^{(1)}\dots g^{(L-1)}$ , which is the labelling of the partition tree.

### A. Four-state 4PSK trellis codes

To demonstrate the designing method of trellis codes based upon above set partition chain, we first present an example of a 4-state  $3 \times 4$ PSK trellis code. In this case,  $M = 4$  and  $L = 3$ . We use the same notations  $\underline{a}_i$  and  $A_i$  as defined above. Let  $B_1 = b^{(1)}\underline{a}_1 + A_1$ ,  $B_2 = b^{(2)}\underline{a}_1 + A_1$ ,  $b^{(1)}, b^{(2)} \in GF(4)$  and  $b^{(1)} \neq b^{(2)}$ . Let

$$\begin{aligned} C_i &= b^{(1)}\underline{a}_1 + \lambda_i \underline{a}_2 + A_2, \text{ for } i = 0, 1, 2, 3, \\ D_i &= b^{(2)}\underline{a}_1 + \lambda_i \underline{a}_2 + A_2, \text{ for } i = 0, 1, 2, 3, \end{aligned} \quad (18)$$

where  $\lambda_0 = 0$ ,  $\lambda_i = \alpha^{i-1}$  for  $i=1, 2, 3$ , and  $\underline{a}_2$  is a coset representative of  $A_2$  in  $A_1$ . Therefore, the *intra*-symbol distance between  $C_i$  and  $D_j$  is 1, the *intra*-symbol distance between  $C_i$  and  $C_j$  (or  $D_i$  and  $D_j$ ),  $i \neq j$ , is 2, and the *inter*-symbol distance of each  $C_i$  (or  $D_i$ ) is 3 for  $i=0, 1, 2, 3$ . We use a 4-state full-connected trellis code as shown in Figure 3. The cosets  $C_i$  are assigned to the branches leaving the even numbered states, and the cosets  $D_i$  are assigned to the branches leaving the odd numbered states. From the figure, the symbol distance of the trellis code is 3. The information rate is 4/3 bits/symbol.

If we use extended Reed-Solomon codes  $A_i = RS(4, 4-i)$  ( $i=0, 1, 2$ ) and the same coding method as above, we obtain a 8-dimensional trellis code with symbol distance 3 and information rate 1.5 bits/symbol. It is obvious that the product distances of both codes are 8.

### B. Eight-state 8PSK trellis codes

The construction method presented above can be generalized to any *M*PSK trellis codes. Here we give an example of 8PSK trellis code, i.e.,  $M = 8$  and  $L = 3$ . We use the same notations  $\underline{a}_i$  and  $A_i$  as defined as above. Again, let  $B_1 = b^{(1)}\underline{a}_1 + A_1$ ,

$B_2 = b^{(2)}\underline{a}_1 + A_1$ ,  $b^{(1)}, b^{(2)} \in GF(8)$  and  $b^{(1)} \neq b^{(2)}$ . Let

$$\begin{aligned} C_i &= b^{(1)}\underline{a}_1 + \lambda_i\underline{a}_2 + A_2, \text{ for } i = 0, 1, 2, \dots, 7, \\ D_i &= b^{(2)}\underline{a}_1 + \lambda_i\underline{a}_2 + A_2, \text{ for } i = 0, 1, 2, \dots, 7, \end{aligned} \quad (19)$$

where  $\lambda_0 = 0$ ,  $\lambda_i = \alpha^{i-1}$  for  $i=1, 2, \dots, 7$ , and  $\underline{a}_2$  is a coset representative of  $A_2$  in  $A_1$ . Therefore, the intra-symbol distance between  $C_i$  and  $D_j$  is 1, the intra-symbol distance between  $C_i$  and  $C_j$  (or  $D_i$  and  $D_j$ ),  $i \neq j$ , is 2, and the inter-symbol distance of each  $C_i$  (or  $D_i$ ) is 3 for  $i=0, 1, 2, \dots, 7$ . We use a 8-state full-connected trellis code as shown in Figure 4. The cosets  $C_i$  are assigned to the branches leaving the even numbered states, and the cosets  $D_i$  are assigned to the branches leaving the odd numbered states. From the figure, the symbol distance of the trellis code is 3. The information rate is 2.0 bits/symbol. Because the mapping is not linear (The addition over  $GF(8)$  does not correspond to addition modulo 8.), it is not clear that one may or may not maximize the product distance. For the time being, an exhaustive search may be used to select  $b^{(i)}$  ( $i=1, 2$ ) such that the minimum product distance in all  $C_i$  and  $D_i$  is maximized. However, the product distance of the code is at least  $64 \sin^6(\pi/8) = 0.20$ .

To extend this example, we notice that, for any  $3 \leq L \leq M$ , the partition  $RS(L, L)/RS(L, L-1)/RS(L, L-2)$  can be used instead of  $RS(3, 3)/RS(3, 2)/RS(3, 1)$ . Therefore, we can construct a trellis code with symbol distance 3 using the same method. In this case, each transition in trellis diagram represents  $8^{L-2}$  parallel branches. The information rate of the trellis code is  $3(L-1)/L$  bits/symbol.

Further extending above results, we can obtain codes with larger symbol distance. The main idea is that, instead of using partition  $GF^L(M) = RS(L, L)/RS(L, L-1)/\dots/RS(L, 1)/\{0\}$ , we use  $RS(L, L-1)/RS(L, L-2)/\dots/RS(L, 1)/\{0\}$ . Then the

same procedure of coding can be used, and the resultant code has symbol distance 4 and the information rate  $3(L - 2)/L$  bits/symbol. Particularly, for  $L = 6$ , the information rate is 2.0 bits/symbol.

Although the above codes have the maximized symbol distances, for  $M \geq 8$ , the product distances of these codes are small. These codes are not good at low (even at moderate) SNR. However, the QPSK codes have both large symbol distances and product distances.

### 3 Constructions of Multi-level Codes for Fading Channels

For AWGN channel codes, the optimum multi-dimensional trellis codes have been found by computer search [15]. However, suboptimal (even some optimum) codes can be designed by hand using the multi-level coding scheme [13]. For the fading channel codes, this situation becomes more complicated. If one uses the design rules [7, 8] in which the symbol distance is maximized first, then choose the code with the maximum product distance among the codes with the maximized symbol distance, the codes constructed in last section would be optimum. But the small product distance severely affects the performance of the codes. In fact, for two codes  $C_1$  and  $C_2$ , if the symbol distance of  $C_1$  is 1 larger than that of  $C_2$ , but the product distance of  $C_1$  is much less than that of  $C_2$ , then  $C_2$  may outperform  $C_1$ . Therefore, even use computer search, we can not guarantee to find the optimum multi-dimensional codes for fading channel. On the other hand, the multi-level coding scheme allows one coordinate all parameters of a code such that any parameter does not severely degrade the performance of the code.

Another advantage of the multi-level codes is that these codes can be decoded either by one stage optimum decoding algorithm or by multi-stage decoding algorithm. The choice of the decoding algorithm should be made such that the best trade-off between coding gain and complexity is achieved. In the following, we will construct several classes of multi-level codes which have performance/complexity advantage over previously known codes.

### A. Two-dimensional Multi-level Codes

A three level coding scheme for 8PSK is shown in Figure 5, where each output bit of  $C_i$  is mapped into the  $i$ th bit of the label of a 8PSK signal point. (The 0th bit is the least significant bit, and the 2nd bit is the most significant bit.) Let  $d_i$  be the Hamming distance of  $i$ th component code  $C_i$ , and  $\delta_i$  be the intra-set (squared Euclidean) distance at partition level  $i$ , for  $i = 0, 1, 2$ . It can be proved that the overall code has the parameters:

$$\delta_H = \min \{d_i, 0 \leq i \leq 2\} \quad (20)$$

$$\Delta_p^2 = \Delta_k^{d_k} \quad (21)$$

where  $k$  satisfies  $d_k = \delta_H$  and  $\Delta_k = \min \{\delta_i, d_i = \delta_H\}$ .

The trellis structure of the overall code can be formed by taking the direct product of trellises of component codes follows. Denote  $\beta_i$  as the trellis of component code  $C_i$ . If the number of signal points associated with one branch transition of each trellis  $\beta_i$  is the same, then the trellis of the overall code is all of the state transitions  $(S_1, S_2, S_3) \rightarrow (S'_1, S'_2, S'_3)$ , where  $S_i \rightarrow S'_i$  is the state transition of  $\beta_i$ . And the output of the multi-level code during the state transition is the direct product of all output of the component codes. If one of the component codes is a block code, the state transition is period time variant (see next example).

Example 3.1 The three component codes are as follows:  $C_1$  is a 4-state rate-1/2 convolutional code,  $C_2$  and  $C_3$  are a single-parity-check code  $(2N, 2N-1, 2)$ . Then the three-level code has symbol distance 2, product distance 4, and information rate  $(5N-2)/2N$  bits/symbol. In this case, the second and third codes have a two-state trellis structure whose one state transition corresponds to one symbol (Figure 6 (a)). To form the trellis of the overall code, we rewrite the trellis of the second and third codes as Figure 6 (b). Each state transition has two parallel branches which corresponds to two signal symbols. The trellis of overall code has  $16$  states with period  $N$  branches ( $2N$  symbols) and four parallel branches in each transition. Because this code has high information rate, it can be used as inner code for bandwidth efficient concatenated coding scheme.

To obtain such codes with larger symbol distance, we may use high rate block and convolutional codes at the second and third level. Thus, the optimum decoding becomes more complicated, and the multi-stage decoding can be used in such case. However, the performance degradation due to multi-stage decoding becomes more severe as the minimum Hamming distances of component codes increase. Roughly speaking, this is because the increase of effective path multiplicity by multi-stage decoding is exponentially proportional to the increase of the Hamming distances of the component codes (see [12, 13]). To avoid the large effective path multiplicity, we may use two-level codes based on partition 8PSK/BPSK which has been used for AWGN codes [14].

Example 3.2 The coding scheme is shown in Figure 7. The first component code is a 4-state rate-1/2 convolutional code, and the second code is a  $(2N, 2N-1, 2)$  block code. The coding scheme is shown in Figure 7. This code have symbol distance 2 and information rate  $1+(2N-1)/2N$ .

To construct such a code with larger symbol distance, we have to increase the symbol distance at each level. High rate block codes or convolutional codes may be used in the second level. The decoding complexity of such a code is moderate because the number of states of a high rate code with Hamming distance equal to or greater than 3 is too big. On the other hand, if we use above three-level structure, to obtain a code with symbol distance 3 or larger, the number of states using optimum decoding at least equals  $4 \times 4 \times 4 = 64$ . Such a code is inferior to the one-level 64-state trellis code [7] with symbol distance 4. To obtain a code with symbol distance 3, a moderate product distance and small number of states, we will use a multidimensional multi-level coding scheme in the next subsection.

### B. Multi-dimensional Multi-level trellis codes

The minimum symbol distance of a multi-dimensional signal set could be larger than 1. Taking this advantage, a multi-dimensional multi-level code can be designed more efficiency than two-dimensional multi-level code. A multi-dimensional multi-level code also can be constructed by several multi-dimensional component codes. In the next example, we will construct a 8-state 8-dimensional code with symbol distance 3 and information rate 2 bits/symbol.

Example 3.3 The coding scheme is shown in Figure 8. The second code is the 4-state eight-dimensional QPSK trellis code constructed in last section with information rate 1.5 bits/symbol. For the convenience of forming the trellis structure, the first component code is a four dimensional binary trellis code with information rate 1/2 bit/symbol which will be described in the next paragraph.

The single-parity-check code (4, 3) is partitioned into 4 cosets by the code (4, 1) as follows:  $A_0 = \{0000, 1111\}$ ,  $A_1 = \{1100, 0011\}$ ,  $A_2 = \{1010, 0101\}$ ,  $A_3 =$

{0110, 1001}. The intra-distance between  $A_i$  and  $A_j$  ( $i \neq j$ ) is 2, and the inter-distance of  $A_i$  ( $i=0, 1, 2, 3$ ) is 4. Using a two-state trellis code whose trellis structure is shown in Figure 9, the resultant code has the minimum Hamming distance 4.

Combing the above two trellis codes, we obtain a 8-state eight-dimensional trellis code with symbol distance 3, product distance 8, and information rate 2 bits/symbol. From Figure 3 and 9, the trellis structure of the overall code is 8-state fully-connected. Each state transition has 32 parallel branches.

The following code is based on the four-dimensional signal set partitioning.

Example 3.4 We use half of the signal points in the  $2 \times 8$ PSK signal constellation and the partition chain of Divsalar and Simon's [5]. A point in  $2 \times 8$ PSK signal set is denoted by a pair of labelling  $[i, j], 0 \leq i, j \leq 7$ . Denote  $\underline{x}_i = [i, 3i(\text{mod}8)], i=0, 1, \dots, 7, E_0 = \{\underline{x}_i, 0 \leq i \leq 7\}, E_i = [0, 2i] \oplus E_0 = \{[0, 2i] \oplus \underline{x}_j, 0 \leq j \leq 7\}, i=1, 2, 3$ , where  $\oplus$  is component-wise addition modulo 8. Denote  $A = E_0 \cup E_1 \cup E_2 \cup E_3, F = \{[0, 0], [2, 6], [4, 4], [6, 2]\}, G = \{[0, 0], [4, 4]\}, H = \{[0, 0]\}$ . Then  $A/E_0/F/G/H$  is a principal partition chain. The coding scheme is shown in Figure 10, where  $C_1$  is a rate-1/2 convolutional code, and  $E_i$  is an  $(n, n-1, 2)$  binary block code,  $i=2, 3, 4$ . Each two output bits of  $C_1$  within one coding interval specifies a coset representative  $[0, 2i]$ , and each element in a codeword of the block codes  $C_2, C_3$  and  $C_4$  specifies a coset representative  $E_0/F, F/G, G/H$ , for  $i=2, 3, 4$ , respectively. The coded sequence is produced by combining the output of these four encoders. Let  $C_1$  be a 4-state trellis code as shown in Figure 11 and  $n = 8$  for  $C_2, C_3$  and  $C_4$ , the overall code has following parameters: symbol distance 3, product distance 2.344, and information rate 1.8125 bits/symbol. For this code,  $l$ -stage (for any  $l \leq 4$ ) decoding can be used. We will discuss the performance and complexity issues in the next section.

## 4 Performance and Complexity

To measure the decoding complexity of a multi-dimensional trellis code, the *normalized branch complexity* was introduced by Ungerboeck [3] and others (e.g., [5]). It can be defined as the number of branch transitions per symbol in the trellis diagram excluding the parallel transitions. For a  $L \times M$ PSK code, if the number of states is  $2^\nu$  ( $\nu$  is the memory of the trellis encoder), and the number of coded bits during a trellis transition interval is  $\tilde{k}$  (i.e.,  $2^{\tilde{k}}$  is the number of branches leaving a given node in the trellis excluding parallel branches), then the normalized branch complexity is  $2^{\nu+\tilde{k}}/L$ , e.g., the normalized branch complexity of the code in Example 3.3 is  $2^{3+3}/4 = 16$  whereas the normalized branch complexity of 8-state Ungerboeck code is  $2^{3+2} = 32$ .

To compare the new codes with previously known codes, both performance and complexity should be considered. For the multi-level codes, if the multi-stage decoding is used, the effective path multiplicity will be greater than the path multiplicity of the code. The effective path multiplicity of a code using multi-stage decoding can be computed as the case of multi-stage decoding for codes on AWGN channel[12, 13]. From the result of multi-stage decoding for codes on AWGN channel, to get benefit of multi-stage decoding, the ratio of effective path multiplicity to the path multiplicity should be small. Let us regard a multi-level code as a two-level code. If the second component code is a high rate code with small Hamming distance, the second component code does not provide much help for the first code when the optimum one-stage decoding is used. In this case, a two-stage decoding can be used, and the performance degradation by the two-stage decoding is small. Here the second component code can also be a multi-level code, and a two-stage (or multi-stage) decoding can be used with additional small performance degradation.

It is very time consuming to compute the upper bound (15) for each code presented above. Instead, we use computer simulation to predict the performance of these codes on Rayleigh fading channel.

Figure 12 shows the performance of the code in Example 3.1 using optimum and three-stage decoding scheme. The difference between the performance by optimum decoding and that by multi-stage decoding is large at low SNR, but small at high SNR ( $E_b/N_0 = 20.0$  dB).

The simulation results for the code in Example 3.2 is shown in Figure 13, where the length of the block code is 8 and two-stage decoding scheme is used. The decoding complexity of this code is about the same as that of 4-state Ungerboeck code. (The binary  $(N, N-1, 2)$  code can be decoded by Wagner decoding algorithm [13], and its decoding complexity can be ignored.) In the figure, we also give the performance of the 4-state Ungerboeck code. The new code loses a little information rate but achieves much better performance.

Figure 14 shows the performance of the code in Example 3.3. From the construction of this code, the optimum decoding scheme is more suitable than two-stage decoding. The performance of the code in Example 3.3 is better than at  $E_b/N_0 > 13$  dB. As mentioned before, the normalized branch complexity of this code is only half of that of the 8-state Ungerboeck code. In the figure, we also include the simulation results of two other codes: One is the 8-state six-dimensional trellis code constructed in section 2B with  $b^{(0)} = 0$  and  $b^{(1)} = 1$ , and another is Divsalar and Simon's 4-state four-dimensional code with  $R=2.0$  bits/symbol [5]. It turns out that the performance of these codes are worse than that of 8-state Ungerboeck's code although their symbol distance are not less than that of Ungerboeck code. This is because the Ungerboeck

code has better distance spectrum.

For the code in Example 3.4, the optimum decoding is a little more complicated, but the two-stage decoding (One is for trellis code, and another is for block code which consists of three binary block codes.) is straightforward. Figure 15 presents the simulation results of the code in Example 3.4 and a similar code, i.e., only the first component code is replaced by an 8-state convolutional code with generator matrix  $[64, 74]$  ( see pp.330 in [16] ) where the length of the block code at second level is 8. We see that, since the symbol distance of second component code is larger than that of the first one for the code in Example 3.4, improving the first component code can significantly improve the performance of the overall code. In the case for which the two-stage decoding scheme is used, the second component code dominates the decoding complexity. Therefore, the modified code only increases a little decoding complexity. The normalized branch complexities of these two codes are  $(2^{2+1} + 2^{3+3})/2 = 36$  and  $(2^{3+1} + 2^{3+3})/2 = 40$ , respectively.

Since the second component code is composed of three binary codes, the decoding complexity of the block code can be further reduced by two or three stage decoding for the block code. Figure 16 gives the simulation results of the BER of the code by two, three and four stage decoding, respectively. From the figure, we can see that the difference between two-stage decoding and three-stage decoding can be ignored at high SNR, and the difference between two-stage and four-stage decoding is small. Since each binary single parity check code can be decoded by the Wagner algorithm, their decoding complexity is very small (much smaller than two-state trellis decoding complexity at high SNR). The decoding complexity of the first trellis code is half of that of Divsalar and Simon's 4-state four-dimensional trellis code mentioned before. Therefore, the total decoding complexity of the new code by four stage decoding can

be considered to be the same order of that of the Divsalar and Simon's code. The new code has smaller information rate (1.8125 v.s. 2.0 bits/symbol). But from the simulation results shown in Figure 17, it saves 3.2 dB at BER of  $10^{-4}$ , and more coding gain can be achieved at lower BER.

## 5 Conclusions

We have proposed two classes of multi-dimensional trellis codes for fading channels. One is based on a new  $M$ -way set partition chain for the  $L \times M$ PSK ( $L \leq M$ ) signal set which maximizes the symbol distance of each subset at each level. Some multi-dimensional trellis codes with symbol length 3 and 4 have been given as examples of codes constructed based on this set partition chain. These codes can achieve very high information rates and are asymptotically optimum for fading channel. However, for  $M \geq 8$ , the product distances of these codes are small.

Multi-level coding scheme can be used to construct codes for fading channels if the partition chain and component codes are properly chosen. A number of examples of multi-level codes have been given. The performance degradation of multi-stage decoding has been considered in the designing of multi-level codes. Simulation results show that these codes have very good performance with small decoding complexity.

## References

- [1] J. L. Massey, "Coding and Modulation in Digital Communications", *Proceedings of the 1974 Int. Zurich Seminar on Digital Commun.*, Zurich, Switzerland, March 1974, pp. E2(1)-(4).

- [2] G. Ungerboeck, "Channel coding with multilevel/phase signals", *IEEE Trans. Inform. Theory*, vol. IT-28, pp. 55-67, Jan. 1982.
- [3] G. Ungerboeck, "Trellis-coded modulation with redundant signal sets; Part I: Introduction; Part II: State of the art", *IEEE Commun. Mag.*, vol. 25, pp.5-21, Feb. 1987.
- [4] D. D. Divsalar and M. D. Simon, "The design of trellis coded MPSK for fading channels: performance criteria", *IEEE Trans. Commun.*, vol. COM-36, pp.1004-1012, Sept., 1988.
- [5] D. D. Divsalar and M. D. Simon, "The design of trellis coded MPSK for fading channels: set partitioning of optimum code design", *IEEE Trans. Commun.*, vol. COM-36, pp.1013-1022, Sept., 1988.
- [6] D. D. Divsalar and M. D. Simon, "Trellis coded modulation for 4800-9600 bits/s transmission over a fading mobile satellite channel", *IEEE J. Select. Areas Commun.*, vol. SAC-5, no.2, pp.162-175, Feb., 1987.
- [7] C. Schlegel and D. J. Costello, Jr., "Bandwidth efficient coding for fading channels: code construction and performance analysis", *IEEE J. Select. Areas Commun.*, vol. SAC-7,
- [8] B. Vucetic and J. Nicolas, "Performance of M-PSK trellis codes over nonlinear fading mobile satellite channels", submitted to *IEEE Trans. on Commun.*, 1989.
- [9] S. G. Wilson and Y. S. Leung, "Trellis-coded phase modulation (MTCM) performance on Rayleigh channels", *Proc. 1987 Int. Conf. Commun.*, Seattle, WA, June 7-10, 1987, pp.21.3.1-5.

- [10] J. K. Wolf, "Efficient maximum likelihood decoding of linear block codes using a trellis", *IEEE Trans. Inform. Theory*, vol IT-24, pp.76-80, 1978.
- [11] J. Wu and D. J. Costello, Jr., "New Multi-level codes over GF(q)", *IEEE Trans. on Inform. Theory*, to appear.
- [12] J. Wu, D. J. Costello, Jr. and L. C. Perez, "On Multi-level MPSK Codes", *1991 IEEE Int. Symp. on Inform. Theory*, Budapest, June 1991.
- [13] A. R. Calderbank, "Multilevel Codes and Multistage Decoding", *IEEE Trans. on Commun.*, Vol. 37, pp. 222-229, March 1989.
- [14] G. J. Pottie and D. P. Taylor, "Multi-level Codes Based on Partitioning", *IEEE Trans. on Inform. Theory*, Vol. 35, pp. 87-89, January 1989.
- [15] S.S. Pietrobon, R. H. Deng, A. Lafanechere, G. Ungerboeck and D. J. Costello, Jr., "Trellis coded multi-dimensional phase modulation", *IEEE Trans. on Inform. Theory*, Vol. 36, pp. 63-89, January 1990.
- [16] S. Lin and D. J. Costello, Jr. *Error Control Coding: Fundamentals and Applications*, Prentice-Hall, Inc., Englewood Cliffs, New Jersey, 1983.
- [17] B. Vucetic, "Bandwidth efficient concatenated coding schemes for fading channels", *1990 IEEE Int. Symp. on Inform. Theory*, San Diego, Jan., 1990.
- [18] B. Vucetic and S. Lin, "Block coded modulation and concatenated coding schemes for error control on fading channel", AAECC'88, also accepted for publication in *Journal of Discrete Applied Mathematics*, 1991.
- [19] L. Zhang and B. Vucetic, "Multilevel modulation codes for Rayleigh fading channels", *AAECC'91*.

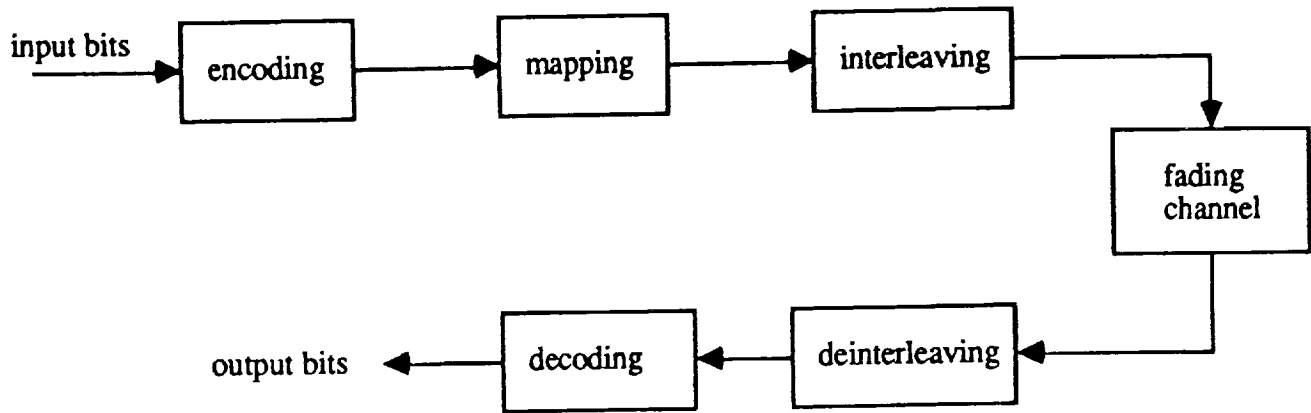


Figure 1 The system model of the coded modulation on fading channel

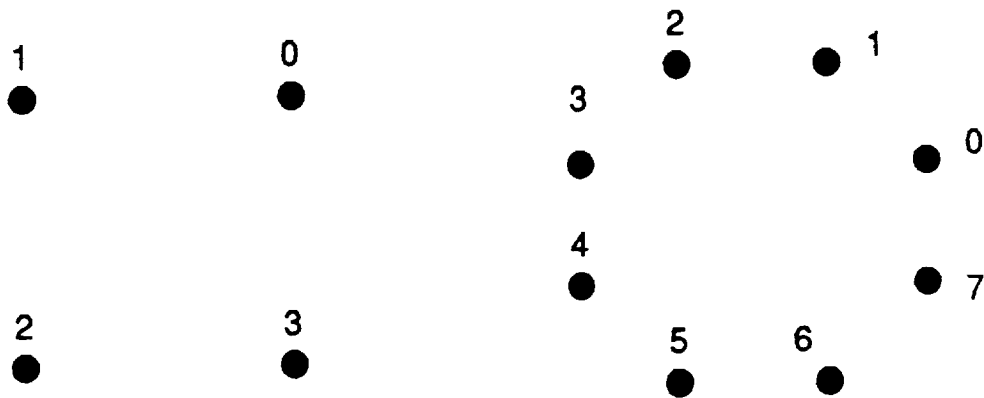


Figure 2 (a) Constellation of QPSK

(b) Constellation of 8PSK

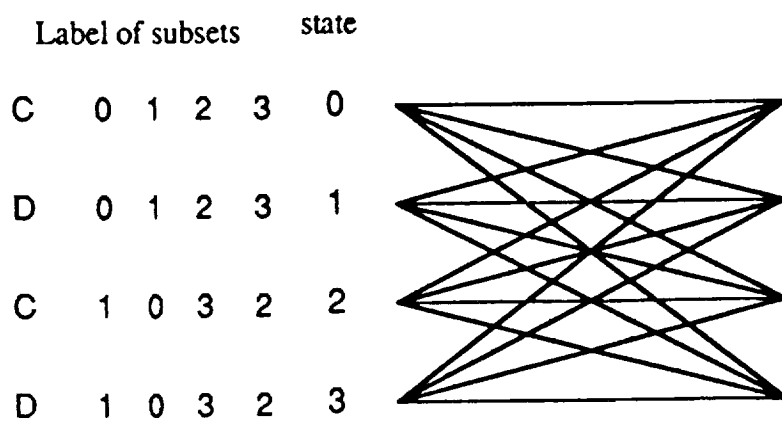


Figure 3 Trellis diagram of 4-state 4-PSK trellis code

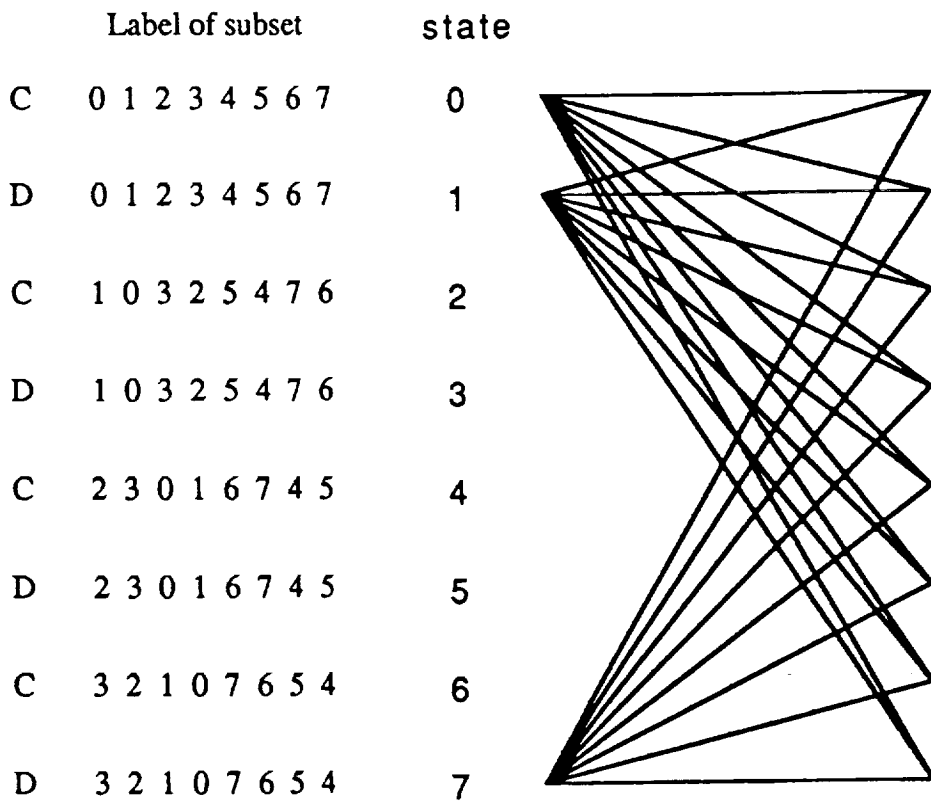


Figure 4 Trellis diagram of 8-state 8-PSK trellis code

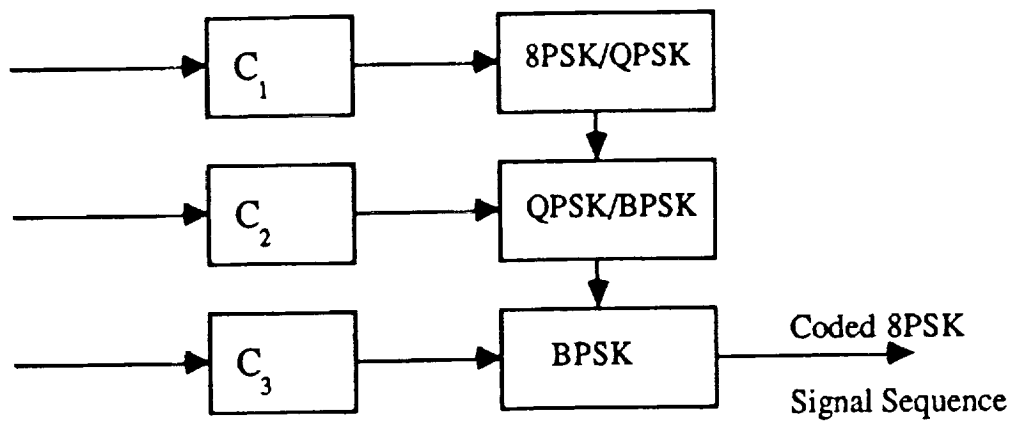


Figure 5 A three-level coding scheme for 8PSK signal set

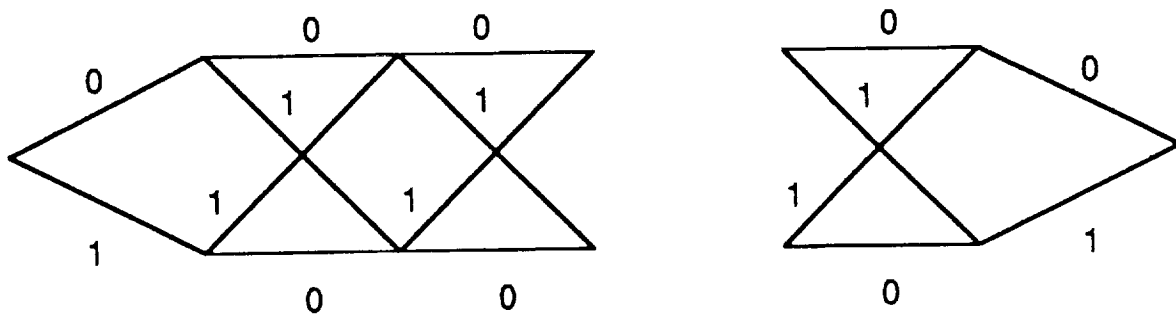


Figure 6 (a) The trellis structure with  $2N$  transitions of  $(2N, 2N-1)$  block code

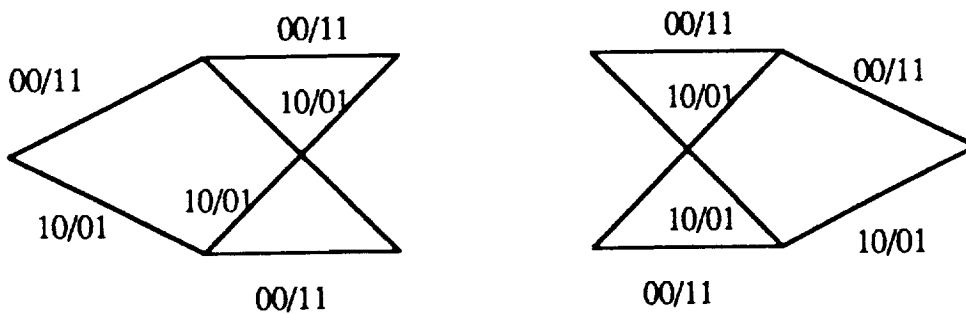


Figure 6 (b) The trellis structure with  $N$  transitions of  $(2N, 2N-1)$  block code

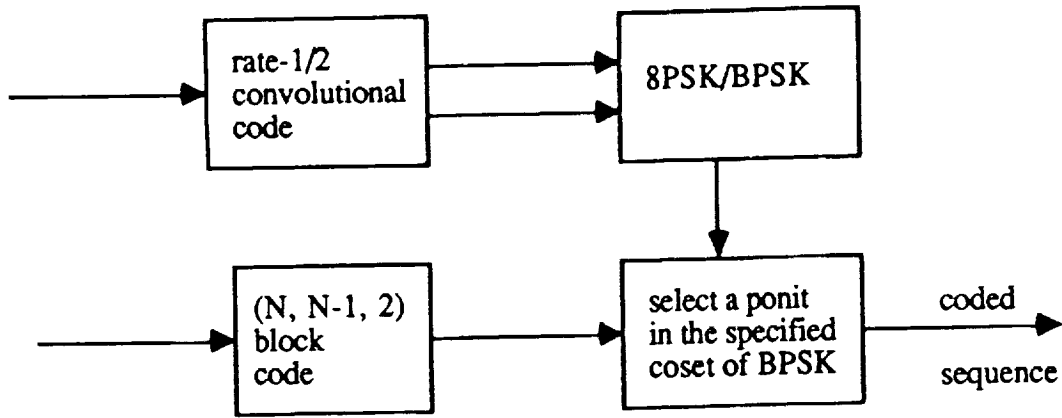


Figure 7 The coding scheme of a two-dimensional two-level code

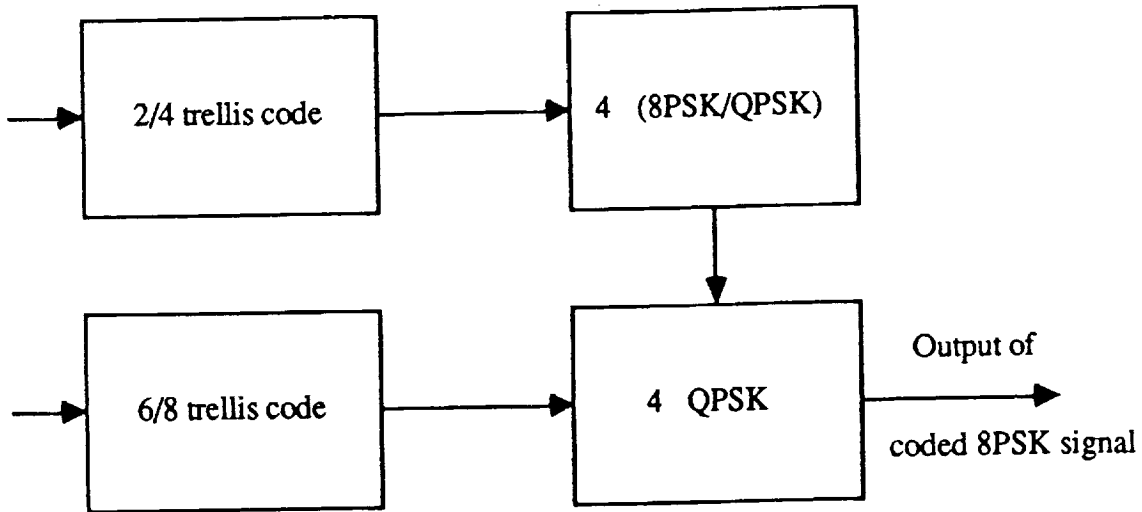


Figure 8 The coding scheme of two-level trellis code

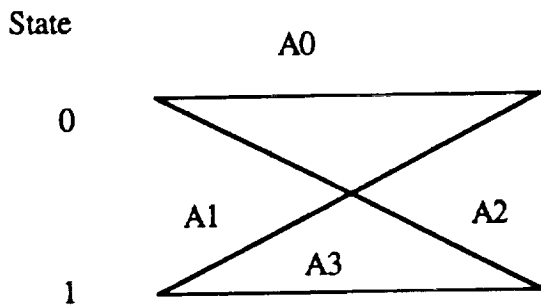


Figure 9 The trellis structure of 2-state rate 1/2 trellis code

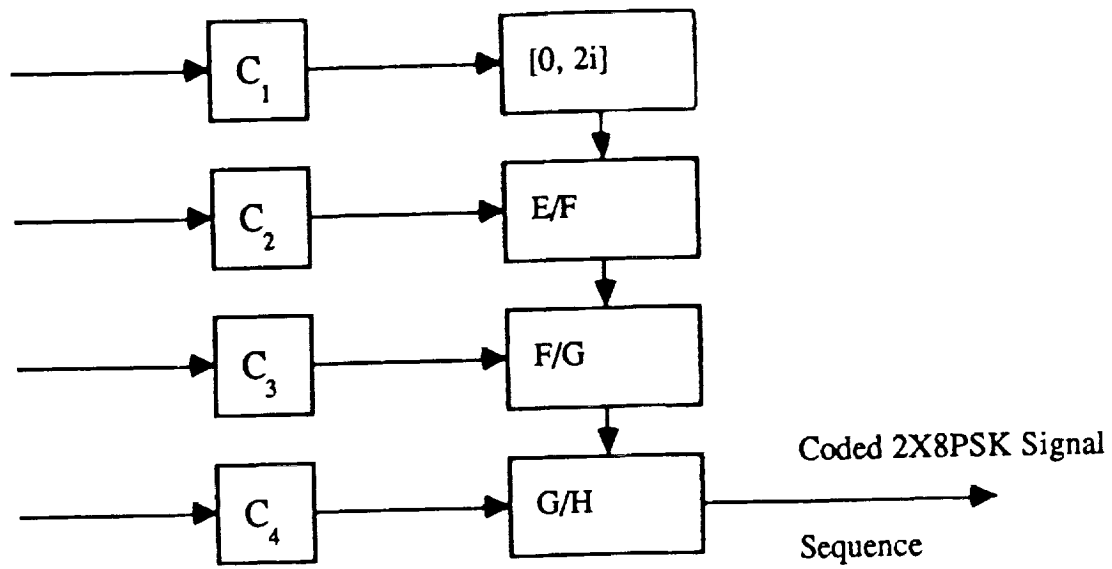


Figure 10 The coding scheme of a four dimensional four-level code

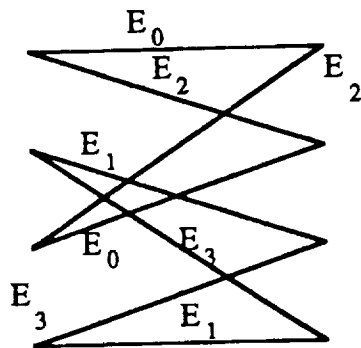


Figure 11 The trellis diagram of  $C_1$  in Example 3.4

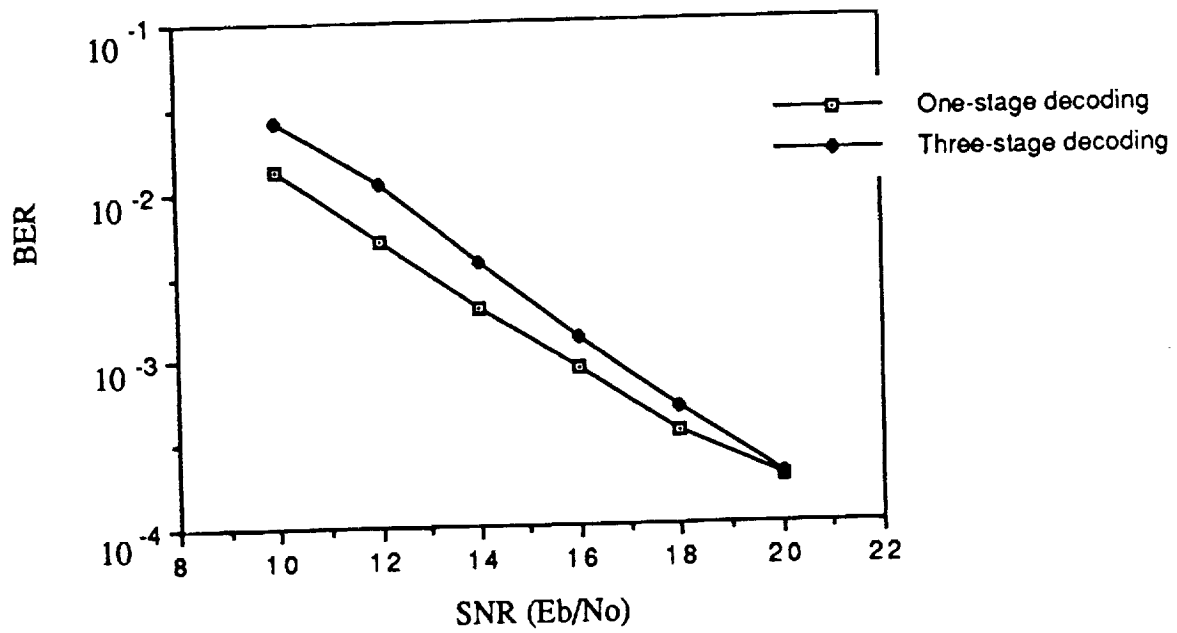


Figure 12 The simulation results of the code in Example 3.1 by one-stage decoding and three-stage decoding, respectively.

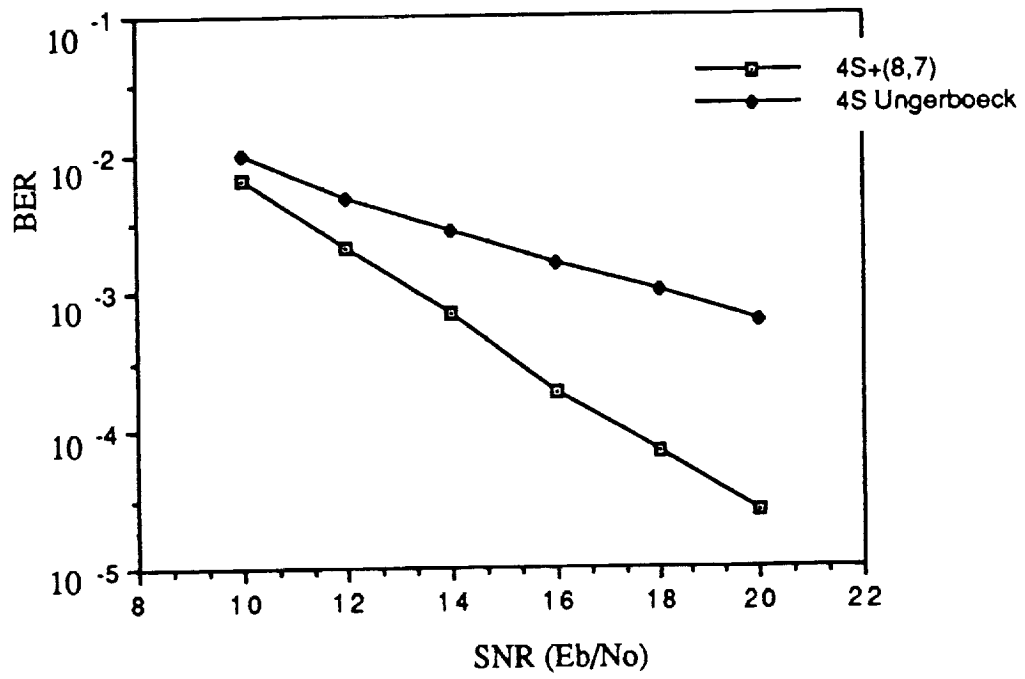


Figure 13 The simulation results of the code in Example 3.2 ( $R=1.875$  bits/symbol) and 4-state Ungerboeck code ( $R=2.0$  bits/symbol)

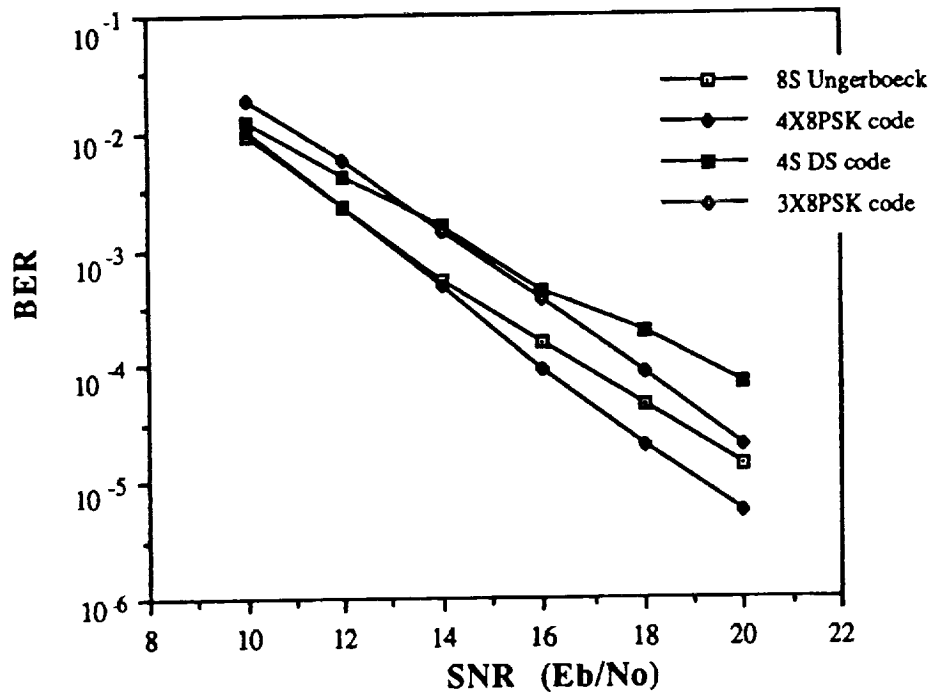


Figure 14 The simulation results of 8-state Ungerboeck code, the code in Example 3.3, 4-state Divsalar and Simon's code and the 8-state six dimensional trellis code in Section 2B

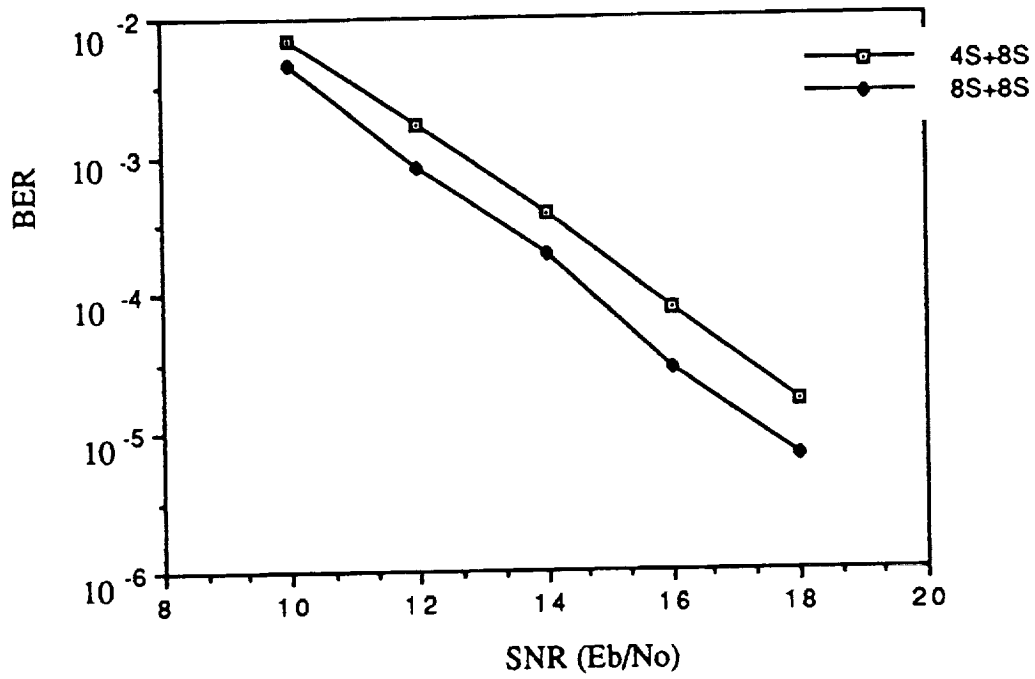


Figure 15 The performance of the code in Example 3.4 and a code whose first component code is 8-state trellis code instead of 4-state trellis code. Both codes is decoded by two-stage decoding.

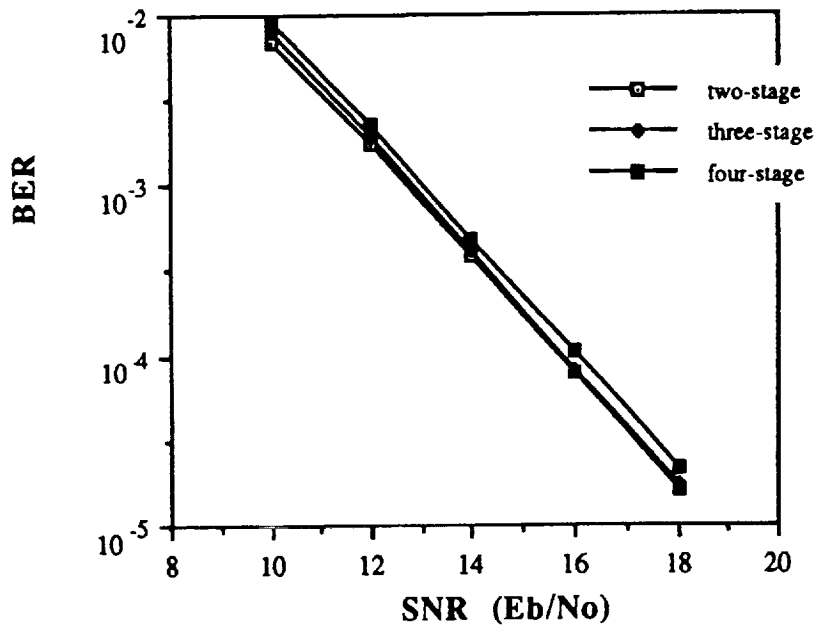


Figure 16 A comparison of the code in Example 3.4 by two, three and four stage decoding.

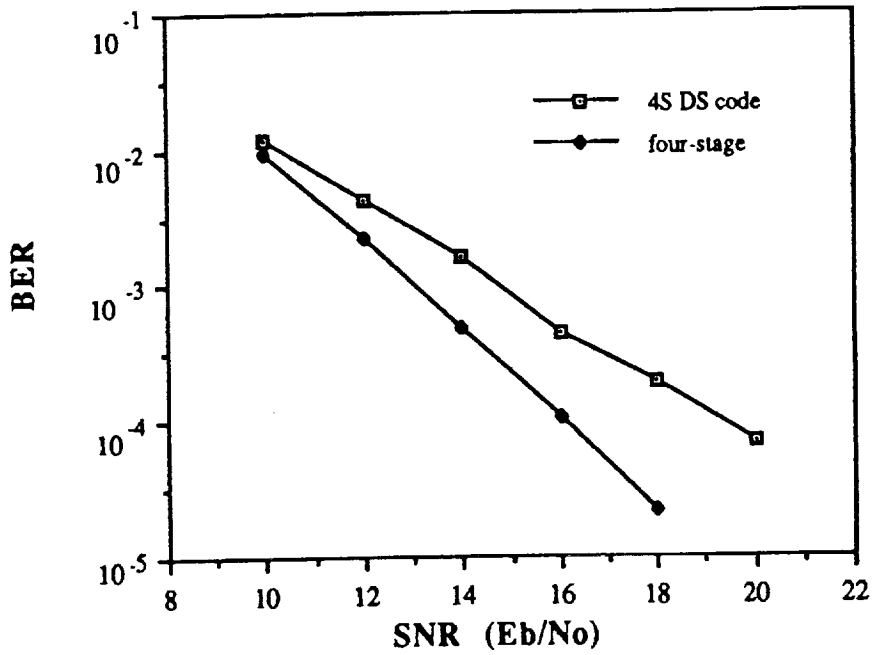


Figure 17 A comparison of the performance of the code in Example 3.4 ( $R=1.8125$  bits/symbol) by four stage decoding with that of 4-state 4-dimensional Divsalar and Simon's code ( $R=2.0$  bits/symbol).